The various low index terminations for monoclinic and hexagonal K_2CO_3 crystals are created along the corresponding crystallographic directions, and shown in Fig. 1S.

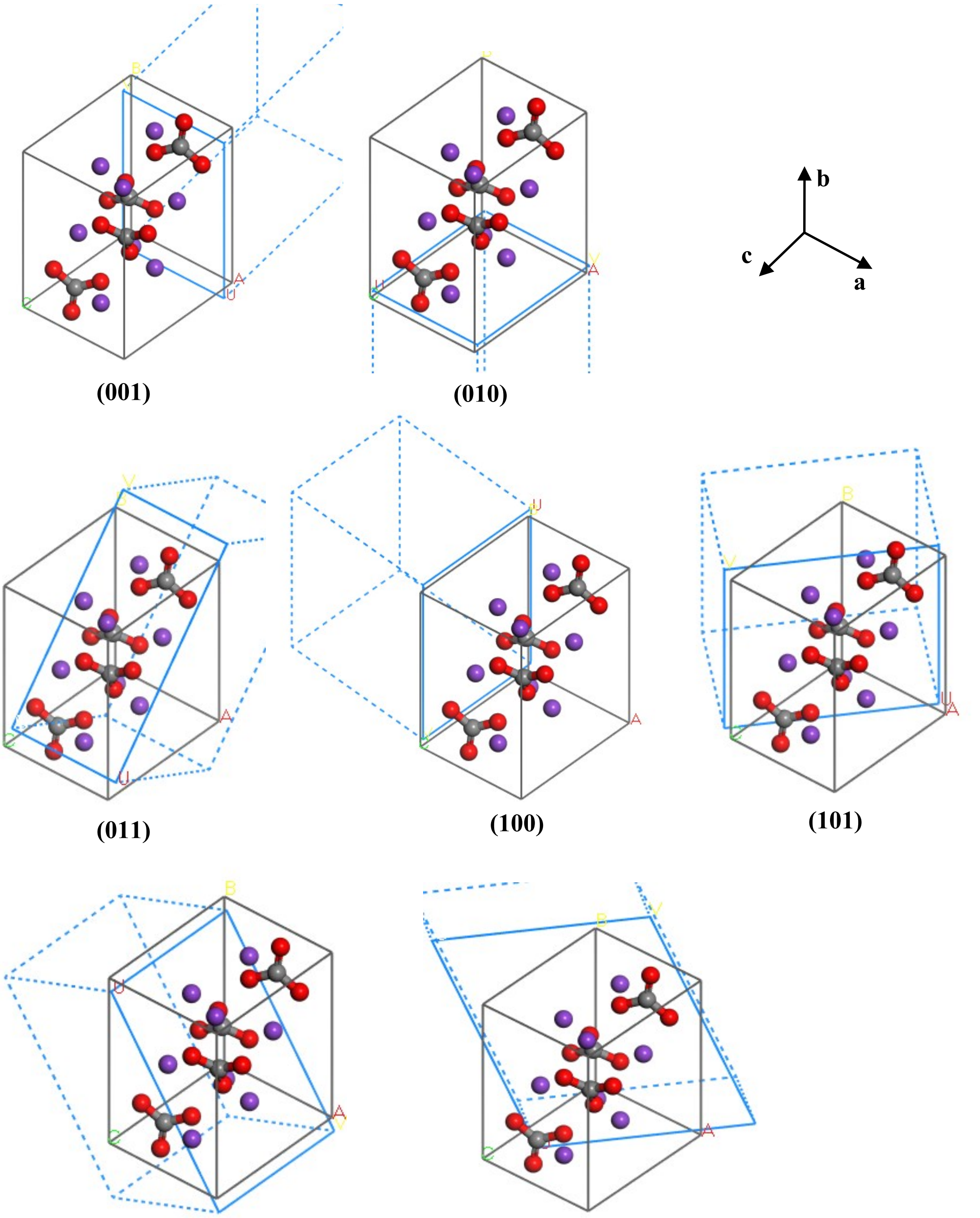

(001) **(010)**

(011) **(100)** **(101)**

(110) **(111)**

(a) The surfaces obtained from monoclinic K_2CO_3.

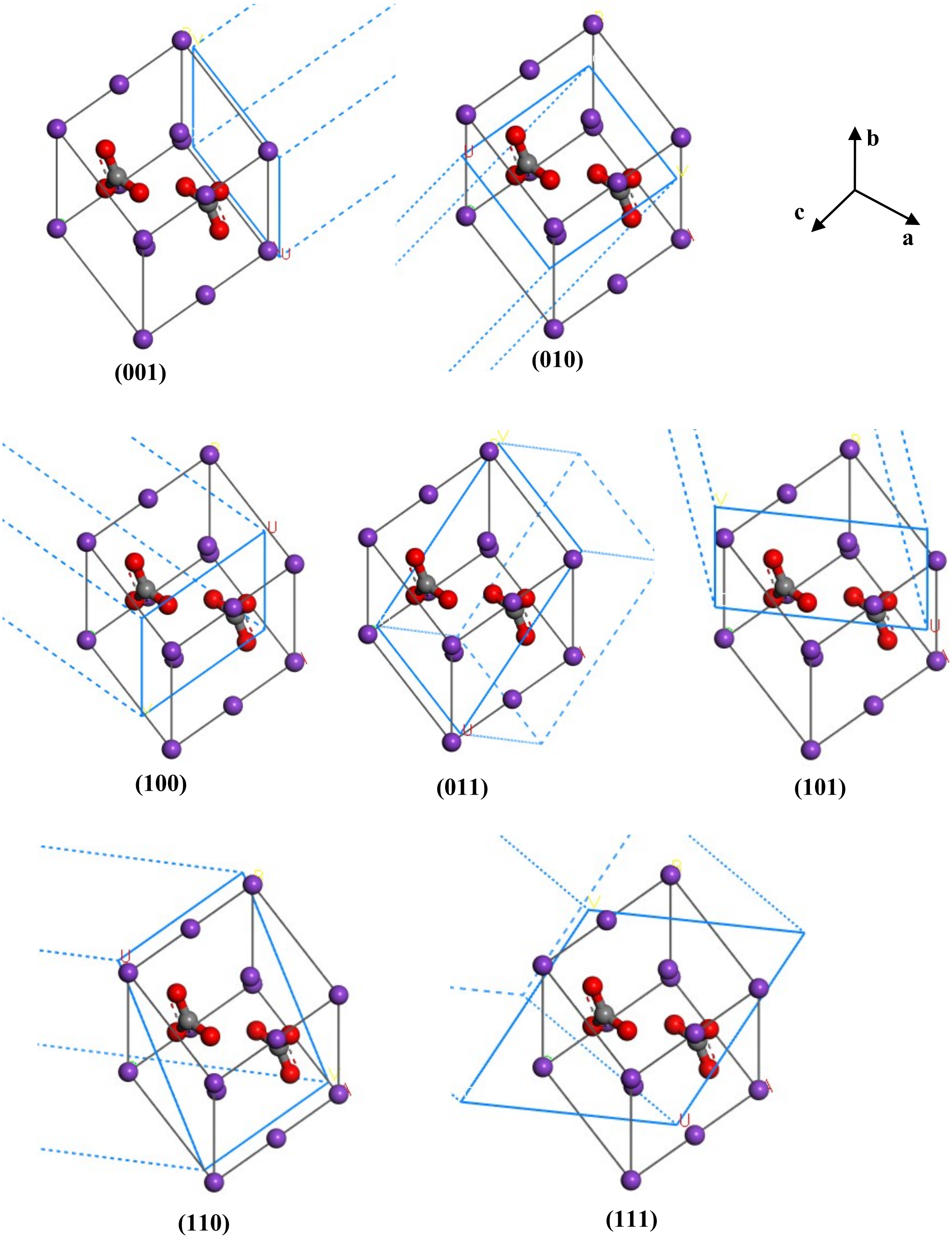

(001) (010)

(100) (011) (101)

(110) (111)

(b) The surfaces obtained from hexagonal K_2CO_3.

Fig. 1S Illustration the cleavage surface from K_2CO_3 crystal(the blue suqare with solid line is the cut surface)

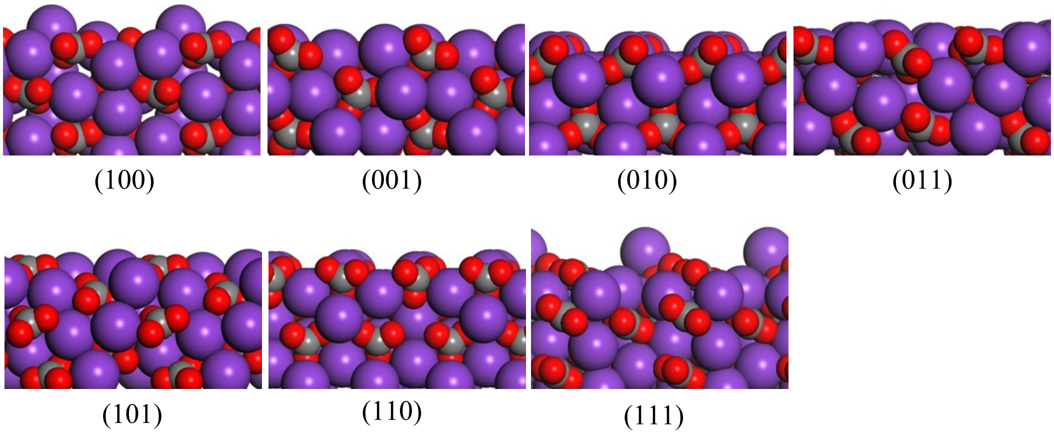

(100) (001) (010) (011)

(101) (110) (111)

(a) Surfaces from monoclinic K_2CO_3

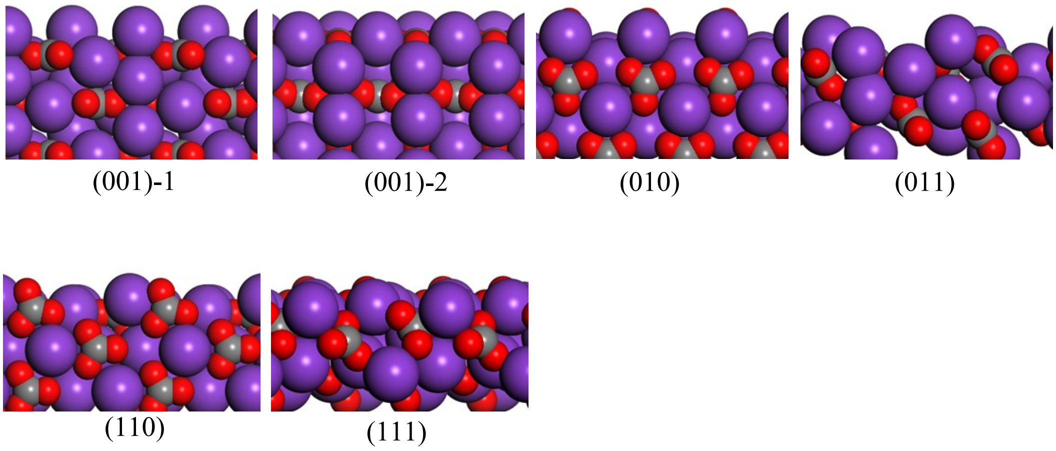

(001)-1 (001)-2 (010) (011)

(110) (111)

(b) Surfaces from hexagonal K_2CO_3

Fig. 2S Side views of the surfaces for K_2CO_3. Red, O; purple, K; and black, C.

K_2CO_3 (001) surface can be viewed as a stacking sequence of two alternating layers, the 1-layer has K^+ and CO_3^{2-}, and 2-layer has row of K^+. Its structure is shown in Fig. 3S.

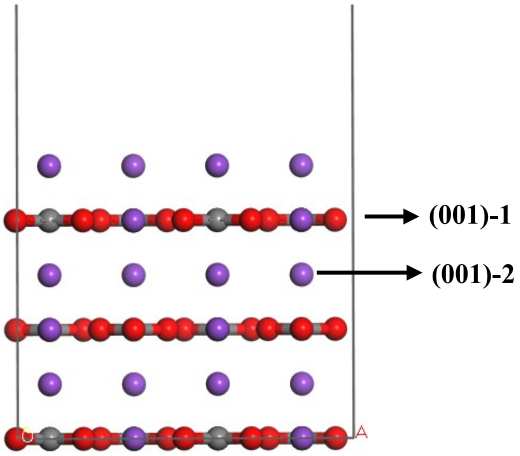

Fig. 3S (001) surface for hexagonal K_2CO_3 and its two different terminations.

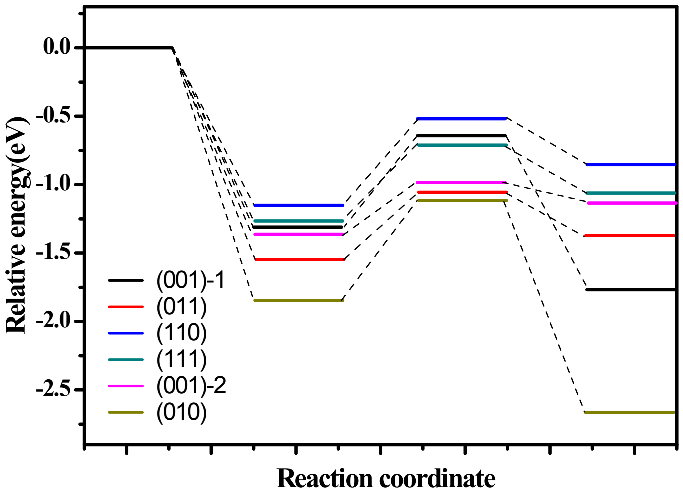

(a) On monoclinic K_2CO_3

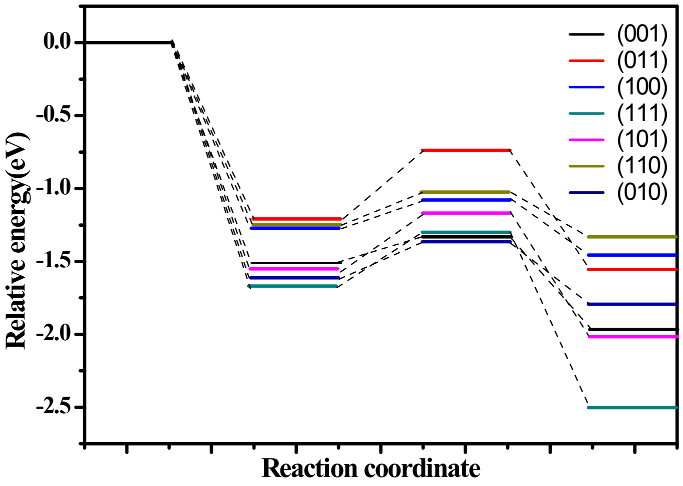

(b) On hexagonal K_2CO_3

Fig. 4S The potential energy of one-step mechanism for carbonation reaction

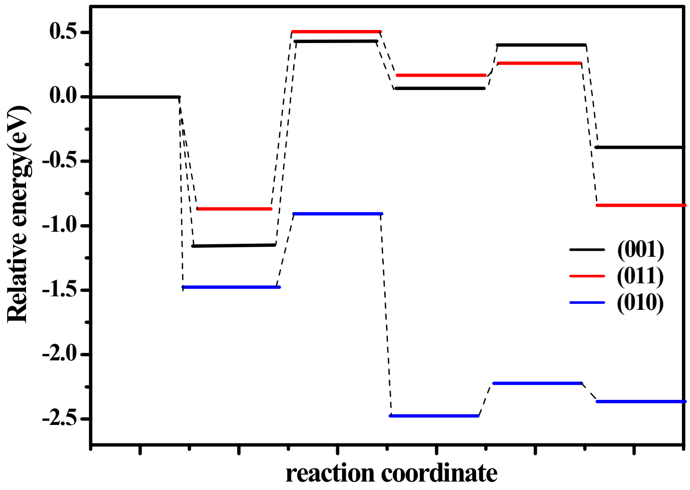

Fig. 5S The potential energy of two-step mechanism for carbonation reaction

Table 1S Calculate values of specific surface energies γ (J m^{-2}) of (100), (001), (010), (011), (101), (110) and (111) surfaces of K_2CO_3 both monoclinic and hexagonal.

structure	layers	5	6	7	8	9	average
monoclinic	(100)	0.364	0.444	0.389	0.456	0.358	0.402
	(001)	0.262	0.263	0.272	0.244	0.272	0.262
	(010)	0.977	0.958	0.999	0.962	0.993	0.978
	(011)	0.315	0.330	0.326	0.374	0.293	0.328
	(101)	0.429	0.441	0.459	0.443	0.428	0.440
	(110)	0.454	0.524	0.425	0.493	0.469	0.473
	(111)	0.379	0.486	0.380	0.481	0.381	0.421
hexagonal	(001)	0.398	0.377	0.520	0.437	0.368	0.420
	(100) (010)	0.946	0.946	0.943	0.944	0.947	0.945
	(101) (011)	0.349	0.389	0.361	0.395	0.346	0.368
	(110)	0.386	0.381	0.393	0.376	0.389	0.385
	(111)	0.366	0.341	0.366	0.355	0.359	0.358

Table 2S Optimized co-adsorption structures and co-adsorption energies (E_{ads}, eV) for CO_2 and H_2O on the monoclinic K_2CO_3 surface.

structure	$d_{C–O1}$	$d_{C–O2}$	$d_{H1–O}$	$d_{H2–O}$	O-C-O	H-O-H	E_{ads}	E_{inter}	*Mulliken charge(e)*	
									CO_2	H_2O
(001)	1.182	1.184	0.974	1.031	176.5	105.9	-1.54	0.01	-0.12	-0.17
(011)	1.183	1.183	0.986	0.992	175.2	99.0	-1.23	-0.03	-0.16	-0.11
(100)	1.176	1.188	1.054	0.977	173.6	105.7	-1.26	-0.06	-0.20	-0.22
(111)	1.180	1.183	0.991	1.011	175.8	101.5	-1.64	-0.05	-0.14	-0.18
(101)	1.179	1.181	0.976	1.066	178.5	106.4	-1.55	0.06	-0.18	-0.24
(110)	1.179	1.184	0.988	0.991	174.2	109.2	-1.24	0.08	-0.08	-0.16
(010)	1.177	1.182	0.991	1.008	178.7	105.1	-1.61	0.26	-0.17	-0.23

Table 3S Optimized co-adsorption structures and co-adsorption energies (E_{ads}, eV) for CO_2 and H_2O on the hexagonal K_2CO_3 surface.

structure	$d_{C–O1}$	$d_{C–O2}$	$d_{H1–O}$	$d_{H2–O}$	O-C-O	H-O-H	E_{ads}	E_{inter}	*Mulliken charge(e)*	
									CO_2	H_2O
(111)	1.188	1.174	1.016	0.976	175.2	108.5	-1.29	0.03	-0.14	-0.19
(011)	1.183	1.198	0.993	1.009	169.9	105.4	-1.55	-0.27	-0.14	-0.20
(110)	1.178	1.184	.978	1.025	178.1	108.6	-1.16	0.09	-0.15	-0.15
(001)-1	1.245	1.253	0.978	1.012	137.0	112.0	-1.31	0.38	-0.69	-0.19
(001)-2	1.188	1.185	0.994	0.999	169.1	99.5	-1.35	-0.22	-0.13	-0.15
(010)	1.173	1.181	1.060	0.978	177.7	110.1	-1.84	-0.09	-0.11	-0.18